Supplementary Information (SI) for Journal of Materials Chemistry A.

Enhanced Thermoelectric and Mechanical Performance of Fully Conjugated Block Polythiophene Modified with Polar Ethylene Glycol Side Chains/Single-Walled Carbon Nanotube Composite Materials

Ye Zhang,[a] Qing Yang,[a] Lin Chen,[a] Roujun Chen,[b] Sunjida Reza Maliha,[c] Yu Chen,[b] Jinjia Xu[c,*] and Chengjun Pan[a,*]

[a] College of Material Science and Engineering, State Key Laboratory of Fine Chemicals, Shenzhen University, Shenzhen 518060, P. R. China. pancj@szu.edu

[b] Key laboratory of Resources Environmental and Green Low Carbon Processes in East Guangdong, School of Chemistry and Environmental Engineering, Hanshan Normal University, Chaozhou, 521041

[c] Department of Chemistry and Biochemistry, University of Missouri-St. Louis, One University Boulevard, St. Louis, MO, 63121, USA. jxbgk@umsystem.edu

Methods

Proton nuclear magnetic resonance (^{1}H NMR) spectroscopy was conducted with Bruker AVANCE III (400 MHz - 600 MHz). Small molecules and polymers were dissolved in $CDCl_3$ (5mg mL^{-1}). Qualitative analysis of the molecular structure of small molecules is achieved through the integration of pertinent peaks in the hydrogen spectra. Quantitative analysis of the block ratio in block copolymers is determined by integrating the area of the terminal methyl groups on the polythiophene side chains.

Gel permeation chromatography (GPC) was performed on Waters e2695 to determine the molecular weight distribution and polydispersity index (PDI) of the polymers and block copolymers. The polymer was dissolved in THF (2 mg mL^{-1}) and filtered by a 0.22 μm membrane to remove undissolved large particles, preventing clogging of the chromatography columns.

Thermogravimetric analysis (TGA) was carried out with TGA-55 to evaluate the thermal stability and decomposition characteristics of the polymers and block copolymers. The sample (10 mg) was heated from 30 °C to 800 °C at a constant heating rate of 10 °C min^{-1} under a nitrogen atmosphere. Defined as the temperature at which the sample loses 5% of its initial weight, indicating the onset of significant thermal degradation.

UV-Visible-Near Infrared Spectroscopy (UV-Vis-NIR) was performed on Lambda 950 instrument to investigate the optical properties and electronic structure of conjugated systems in polymers, particularly focusing on π–π* conjugation. The absorption spectra of the block polythiophene in THF was to understand the electronic transitions in the solution state. Drop-casting method was used to prepare films. The spectral range for films extends from 350 nm to 2000 nm.

Electrochemical Performance Analysis was conducted with CH166E to calculate the electrochemical energy levels by a three-electrode system. Scan the potential range at rate of 300 mV s^{-1}. Working electrode was Platinum rod. Reference electrode was silver chloride electrode (Ag/AgCl). Counter electrode was Platinum wire mesh. Standard Electrode was Ferrocene (Fc) for potential calibration. Prepare a 0.1 M tetrabutylammonium hexafluorophosphate (Bu4NPF6) solution in dichloromethane (DCM). A small amount of the block polythiophene was dissolved in the electrolyte solution. Bubble nitrogen gas through the solution for 30 minutes to remove dissolved oxygen prior to each measurement.

Scanning electron microscopy (SEM) measurements were done with SU-70 to investigate the surface morphology and composition of polymers and block copolymers by collecting secondary electrons (SE) and backscattered electrons (BSE) generated from the interaction of high-energy electron beams with the sample.

Laser Raman Spectroscopy (Raman) was carried out with Renishaw in Via Raman Microscope to provide detailed information about molecular structure and vibrational energy level changes through the interaction of photons with molecules, and use a 514 nm excitation source and scanning the range of 1000 cm^{-1} to 2000 cm^{-1} to analyze films composite with single-walled carbon nanotubes (SWCNTs).

Thermoelectric Parameter testing system in quasi-steady-state mode was performed on MRS-3 to measure electrical conductivity and seebeck coefficient of the thin films at room temperature and variable temperature (300K-500K). Perform each measurement on five samples and calculate the average value for accuracy at room temperature. Maintain vacuum condition conditions throughout variable temperature measurement.

Hall effect measurement system was conducted with HMS-7000 to measure carrier concentration and mobility. The Hall effect is essentially an electromagnetic phenomenon. By applying a magnetic field and current, the resulting potential difference can provide information about the carrier concentration, carrier mobility, and carrier type in semiconductor materials.

X-ray photoelectron spectroscopy (XPS) was carried out with K-Alpha to determine the elemental composition of the sample by analysing the energy of the emitted photoelectrons. For a specific element, the binding energy shifts can provide information about the element's oxidation state. For instance, when an element undergoes oxidation and loses electrons, the increased attraction between the nucleus and the remaining electrons requires higher energy to excite an electron, resulting in an upward shift in binding energy. XPS is used to analyse the electronic structure of and composite films.

Ultraviolet photoelectron spectroscopy (UPS) was performed on ESCALAB 250Xi to study the electronic structure of materials, particularly the valence band region. UPS involves exciting electrons using ultraviolet (UV) light and measuring the kinetic energy of the emitted photoelectrons. This technique provides detailed information about the density of states, work function, and the valence band maximum (VBM) of materials, making it valuable for analysing the electronic properties of thin films, including polymers and block copolymers used in thermoelectric applications.

Tensile and Bending Tests measurements were done with a universal testing machine (UTM) CMT4204 to evaluate the mechanical properties of thin film polymers, including their strength, flexibility, and durability. For the tensile text, composite film specimens were prepared according to the national standard Type 2 dumbbell shape. Secure the dumbbell-shaped specimen in the grips of the UTM, ensuring proper alignment to avoid uneven stress distribution. tensile text was conducting at room temperature by the rate of 0.5mm min^{-1}. For the bending text, thin film specimens were prepared by depositing the composite material onto a polyimide (PI) substrate. Cut the PI substrate with the composite film into strips of 1 cm × 4 cm and use copper foil tape to protect the ends of the film where it contacts the multimeter probes. Ensure good electrical contact by firmly attaching the tape. Use a bending test apparatus that can apply controlled bending to the film with varying curvature radii and record the electrical resistance varation.

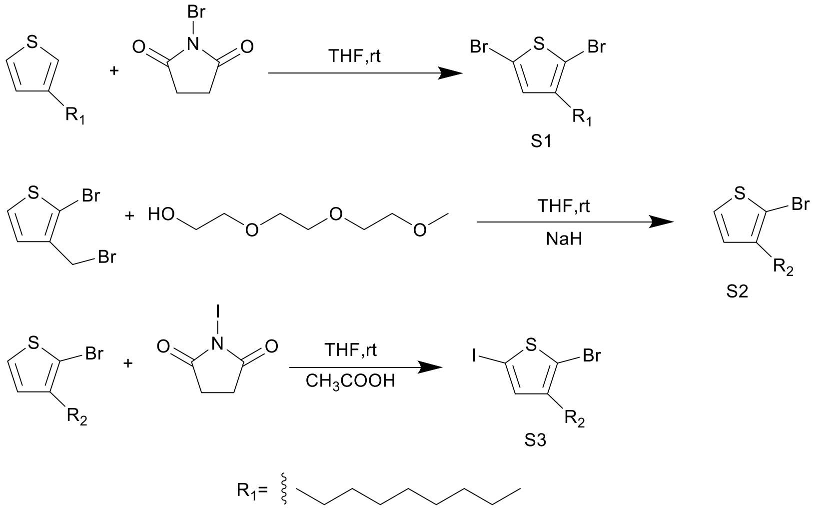

Scheme S1. Synthesis Route of Monomers **S1**, **S2** and **S3**.

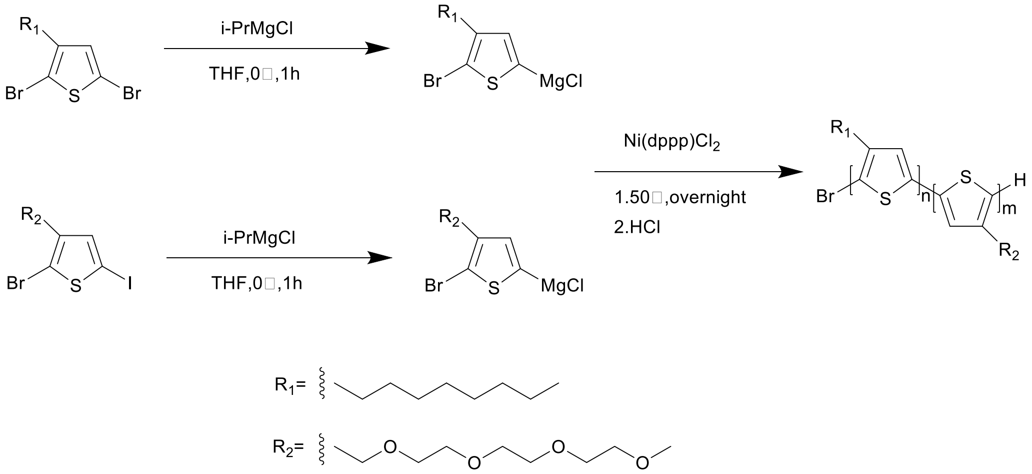

Scheme S2. Synthesis Route for **P3OT-*b*-P3TEGT** Block Copolymer.

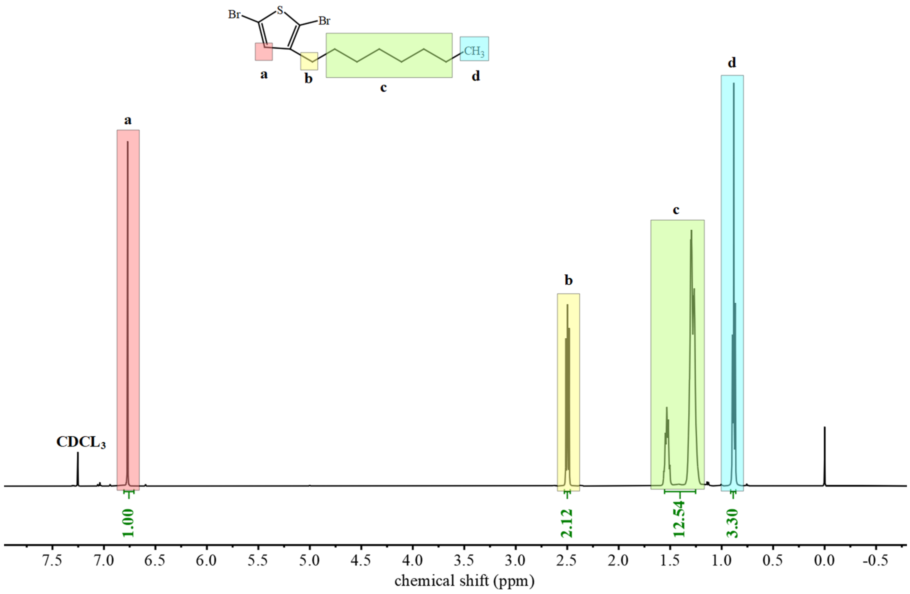

Fig. S1. ^{1}H NMR of **S1** in $CDCl_3$.

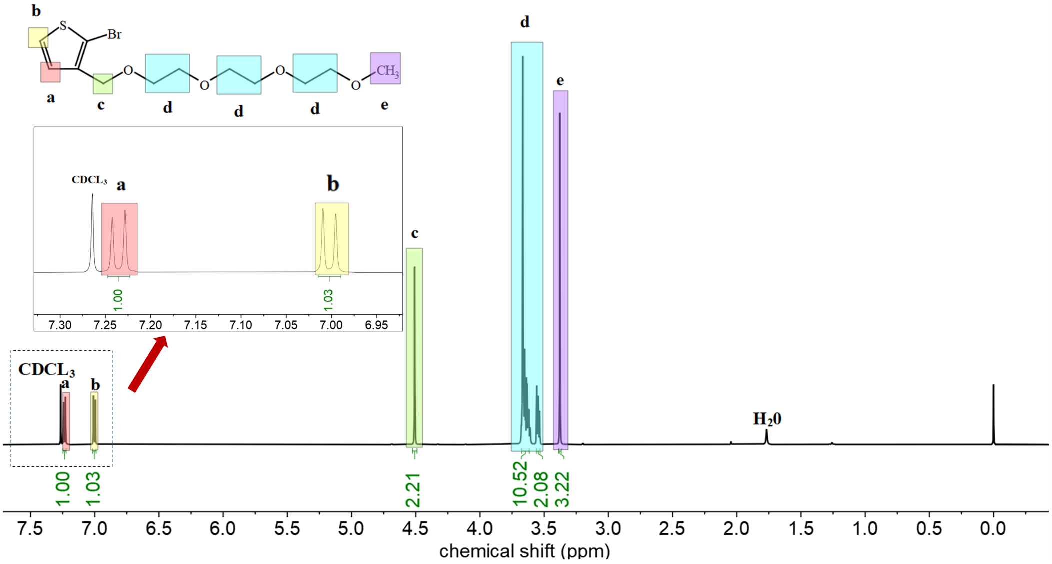

Fig. S2. ^{1}H NMR of **S2** in CDCl$_3$.

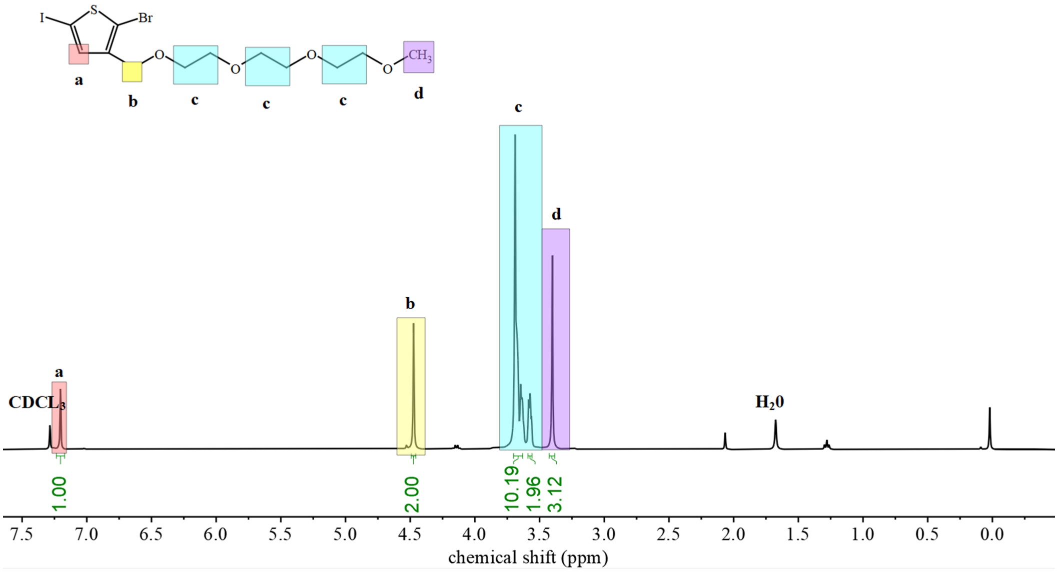

Fig. S3. ^{1}H NMR of **S3** in CDCl$_3$.

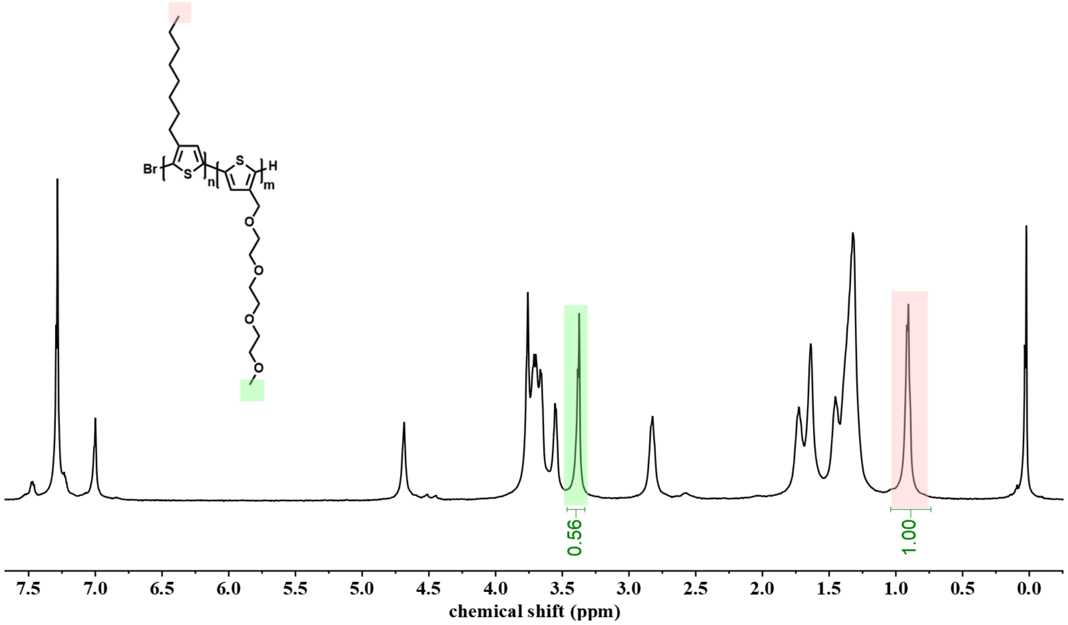

Fig. S4. ^{1}H NMR of **P3OT-*b*-P3TEGT** with a block ratio of 2:1(**P3OT** to **P3TEGT**) in CDCl$_3$.

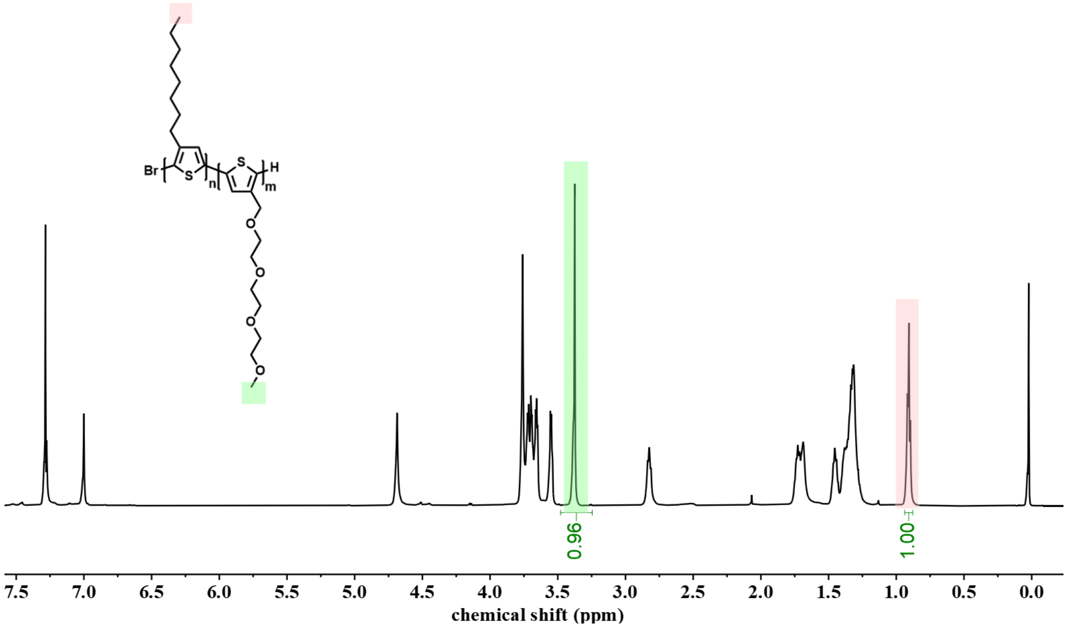

Fig. S5. ^{1}H NMR of **P3OT-*b*-P3TEGT** with a block ratio of 1:1 in CDCl$_3$.

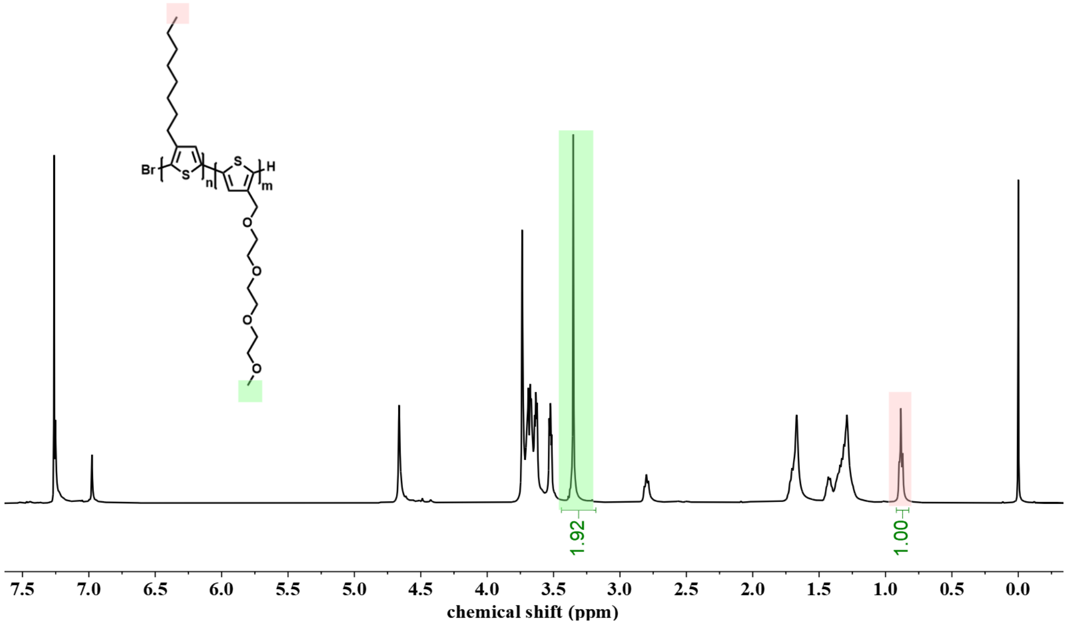

Fig. S6. ^{1}H NMR of **P3OT-*b*-P3TEGT** with a block ratio of 1:2 in $CDCl_3$.

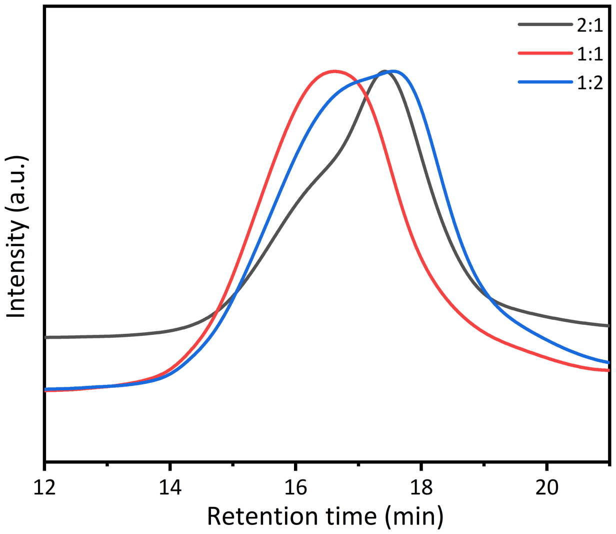

Fig. S7. GPC curve of **P3OT-*b*-P3TEGT** with different block ratios.

Table S1. Molecular Weights and Distributions of **P3OT-*b*-P3TEGT** with Different Block Ratios

Polymer	***Mn*** **[kDa]**[a)]	***Mw*** **[kDa]**[b)]	**PDI**[c)]
P3OT-*b*-P3TEGT-2:1	16.14	19.67	1.22
P3OT-*b*-P3TEGT-1:1	17.39	25.39	1.46
P3OT-*b*-P3TEGT-1:2	13.63	19.99	1.47

[a), b), c)] Obtained from the GPC results, M_n: Number-average molecular weight; M_w: weight-average molecular weight, PDI: polydispersity.

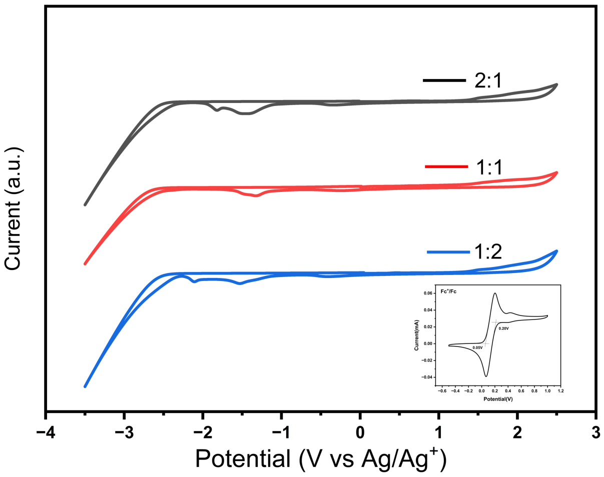

Fig. S8. CV curves of **P3OT-*b*-P3TEGT** with different block ratios.

Table S2. Electrochemical Properties of **P3OT-*b*-P3TEGT** with Different Block Ratios

Polymer	***E_{HOMO}(eV)***	***E_{LUMO}(eV)***	***$E_g^{electro}$ (eV)***
P3OT-*b*-P3TEGT-2:1	-6.13	-3.47	2.66
P3OT-*b*-P3TEGT-1:1	-6.11	-3.43	2.68
P3OT-*b*-P3TEGT-1:2	-6.07	-3.46	2.61

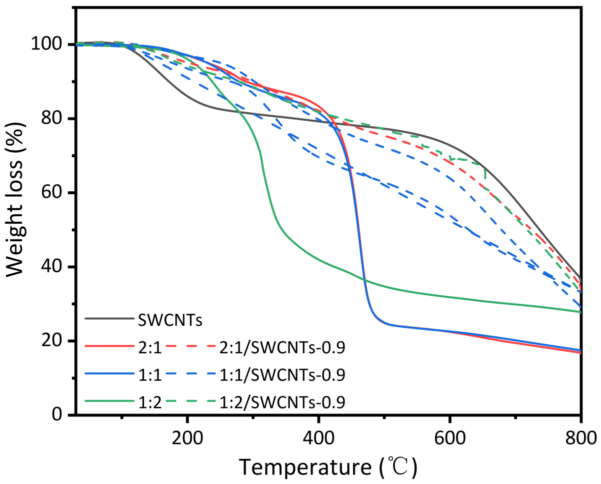

Fig.S9. TGA curves of **P3OT-*b*-P3TEGT** and **P3OT-*b*-P3TEGT**/SWCNTs-0.9.

Table S3. Thermal Decomposition Temperatures of **P3OT-*b*-P3TEGT** and **P3OT-*b*-P3TEGT**/SWCNTs-0.9 with Different Block Ratios

Polymer	$T_{d\ 5\%}$ [°C]$^{a)}$
P3OT-*b*-P3TEGT-2:1	231.79
P3OT-*b*-P3TEGT-1:1	231.03
P3OT-*b*-P3TEGT-1:2	209.27
SWCNTs	141.43
2:1 P3OT-*b*-P3TEGT/SWCNTs-0.9	203.13
1:1 P3OT-*b*-P3TEGT/SWCNTs-0.9	177.58
1:2 P3OT-*b*-P3TEGT/SWCNTs-0.9	187.42

a) Estimated from the TGA curves.

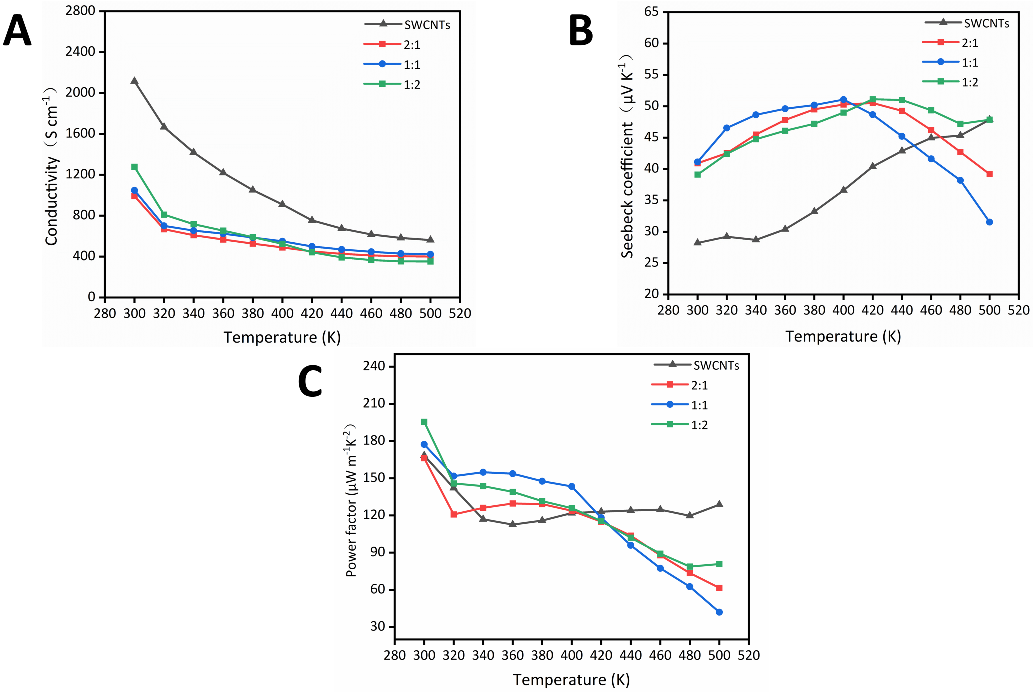

Fig. S10. (A) Electrical conductivity graph of **P3OT-*b*-P3TEGT**/SWCNTs-0.9 at different temperatures; (B) Seebeck coefficient graph of **P3OT-*b*-P3TEGT**/SWCNTs-0.9 at different temperatures; (C) Power factor graph of **P3OT-*b*-P3TEGT**/SWCNTs-0.9 at different temperatures